Electronic Supplementary Material (ESI) for CrystEngComm.
This journal is © The Royal Society of Chemistry 2015

Electronic supporting Information:

A self-catenated *rob*-type porous coordination polymer constructed from triazolate and carboxylate ligands: fluorescent response to the reversible phase transformation

Mingli Deng,[a] Shijun Tai,[b] Weiquan Zhang,[a] Yongchen Wang,[a] Jiaxing Zhu,[a] Jinsheng Zhang,[b] Yun Ling*,[a] and Yaming Zhou [a]

a. Shanghai Key Laboratory of Molecular Catalysis and Innovative Materials, Department of Chemistry, Fudan University, Shanghai, 200433, China.

b. College of Chemistry, Chemical Engineering and Environmental Engineering, Liaoning Shihua University, Liaoning, 113001, China.

Email: yunling@fudan.edu.cn (Ling, Y.)

Fig. S1. the PXRD patterns obtained for synthesis pure phase of **MA-11**. (*Case 1*: 0.02 mL HAC, *Case 2*: 0.06 HNO_3, *Case 3*: 0.06 mL HBF_4, *Case 4*: HNO_3 (0.2 mL) and HBF_4 (0.06 mL), *Case 5*: 0.12 mL HNO_3, *Case 6*: 0.06 mL HNO_3 and 0.06 mLHBF_4)

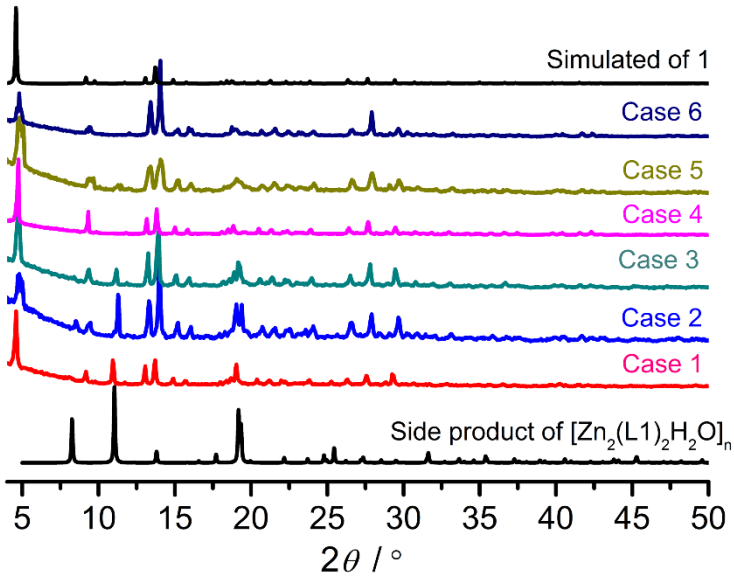

Fig. S2. the crystal structure of the side product obtained without additional acid. (a) the structure motif (A: 2/3-x, 4/3-y, 1/3-z; B: -x+y, 1-x, z; C: 1-y, 1+x-y, z; D: 2/3+x-y, 1/3+x, 1/3-z; E: -1/3+y, 1/3-x+y, 1/3-z; F: 2/3-x, 1/3-y, 1/3-z); (b) the two-dimensional layer structure; (c) the packing structure

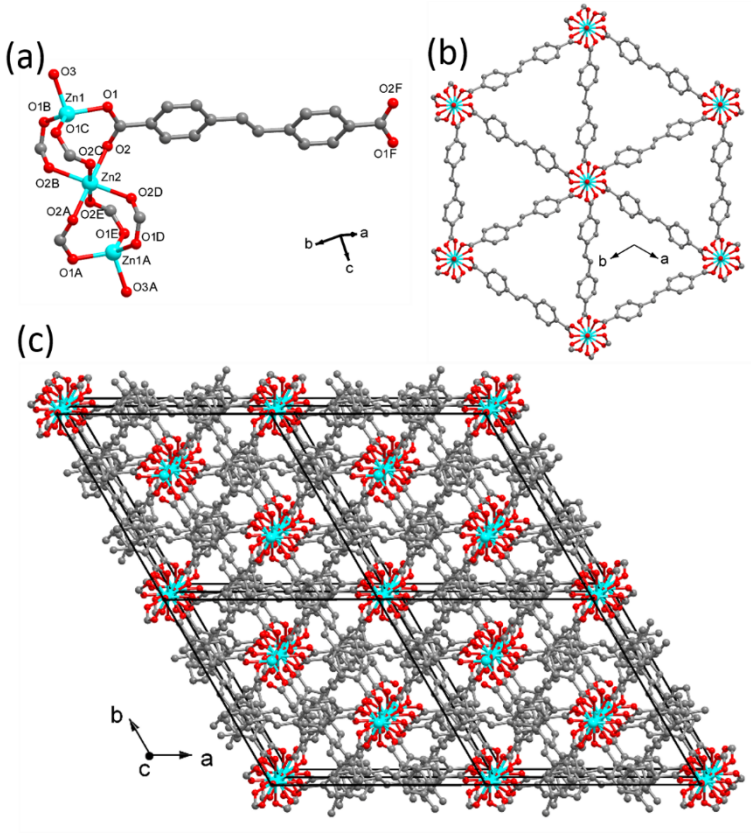

Fig. S3. (a) the structural motif of **MAC-11** with atomic label (symmetry codes: A: 0.5-x, 0.5-y, -z; B: 0.5-x, 0.5+y, 0.5-z; C: x, -y, -0.5+z; D: -x, -y, -z); (b) the three-dimensional structure of MAC-11 showing 1D channel along c axis (the green: Connolly with probe atom radii of 1.4 Å, cell: 1 × 4 × 4); (c) the two-dimensional layer formed exclusively by Zn2(dmtrz)2 dimers (α: the dihedral angle); (d) the rob (48.66.8) net of 1 after considering of Zn2(dmtrz)2 as 6-connected node (the pink and red ring show the self-catenated hopf links).

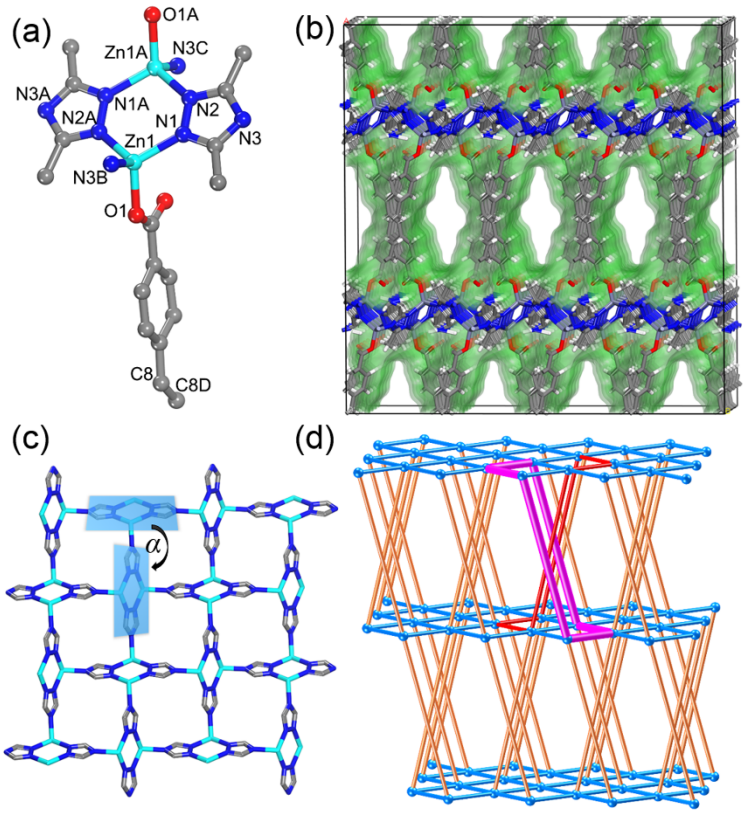

Fig. S4. (a) the structure motif of **MAC-13** (symmetry codes: A: 0.5-x, 0.5-y, -z; B: 0.5-x, -0.5+y, 0.5-z; C: x, 1-y, -0.5+z); (b) the two-dimensional (4,4) layer with the dihedral angle of 82.84°, which is slightly smaller than that in **1**; (c) the three-dimensional structure of 2 showing the accessible porous structure along *c* axis (the green surface: calculated by Connolly method with the probe atomic radii settled to be 1.4 Å).

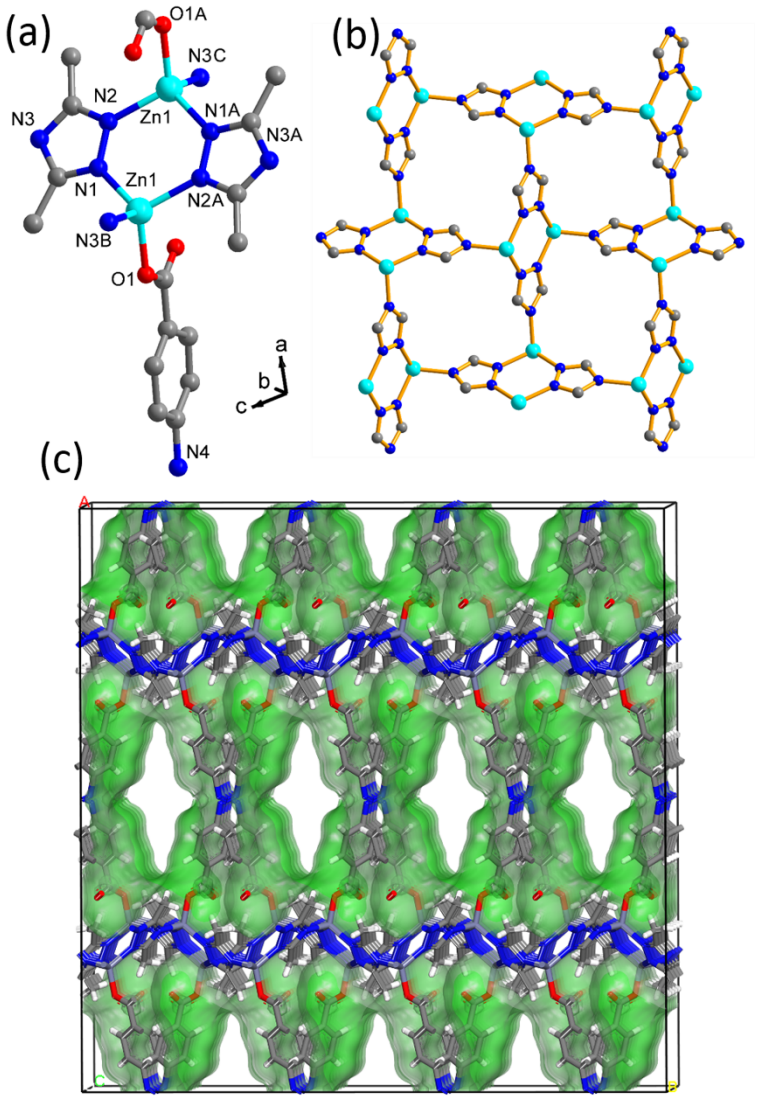

Fig. S5. N_2 sorption isothermal of **MAC-11**, **MAC-13** and **MAC-14** at 77 K

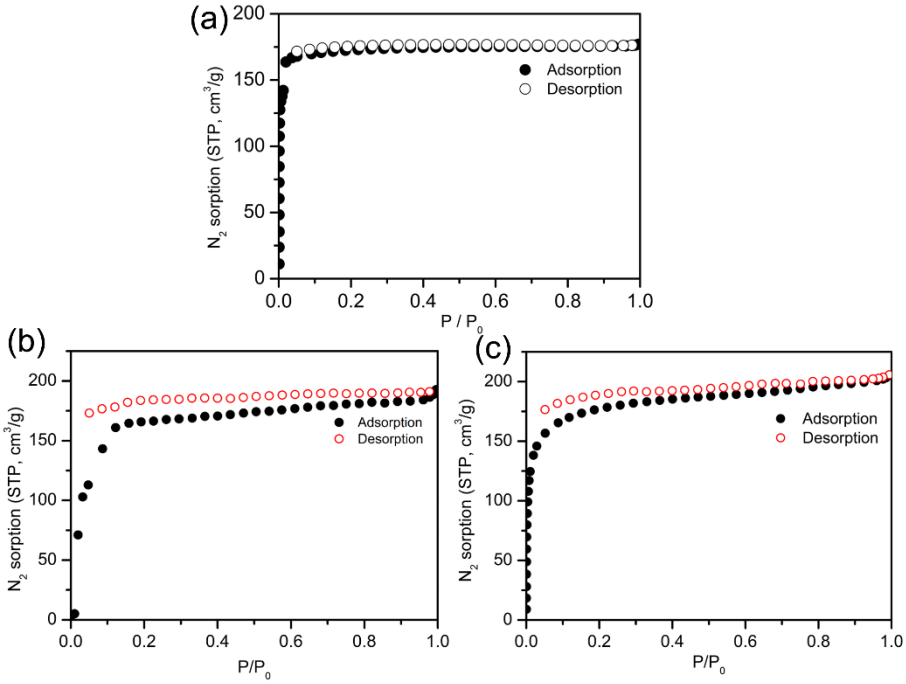

Compound	Surface area (m^2/g)		Pore size	Pore Volume
	BET	Langmuir	(H-K, Å)	(micropore, Å)
MAC-11	722	763	5.9	0.26
MAC-13	719	755	7.8	0.21
MAC-14	677	831	6.9	0.24

Fig. S6. (a) the structure motif of **MAC-14** (symmetry codes: A: 0.5-x, 0.5-y, 1-z; B: x, -y, -0.5+z; C: 0.5-x, 0.5+y, 1.5-z; D: 1-x, y, 0.5-z); (b) the three-dimensional structure of MAC-14 showing the accessible porous structure along *c* axis (the green surface: calculated by Connolly method with the probe atomic radii settled to be 1.4 Å); (c) considering the Zn-dmtrz dimer as a 6-connected node, **MAC-14** can be regarded as 6-connected *pcu*-type framework.

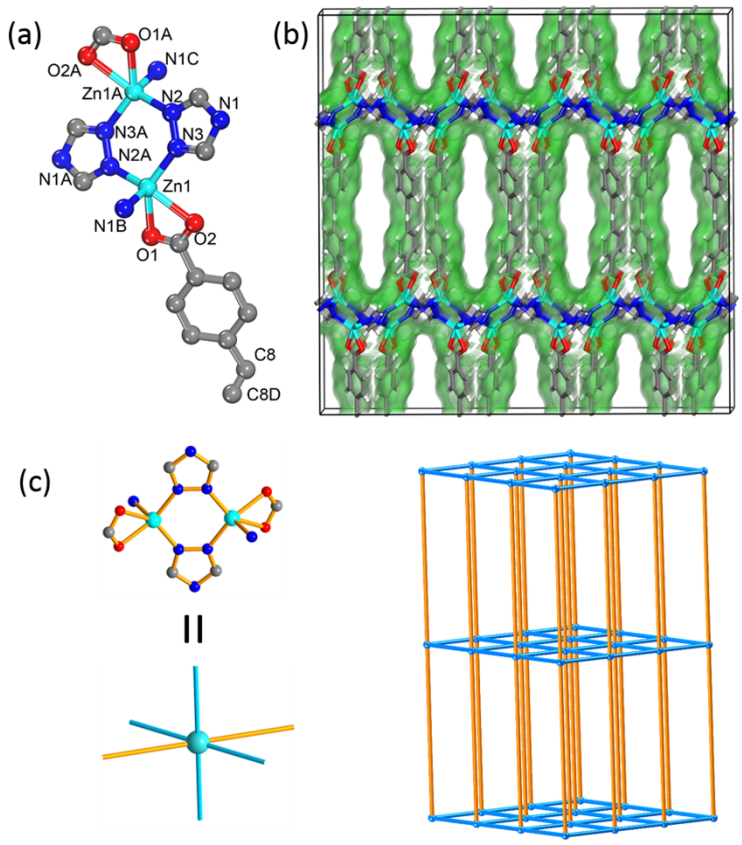

Fig. S7. The PXRD patterns of **MAC-11** in common solvent.

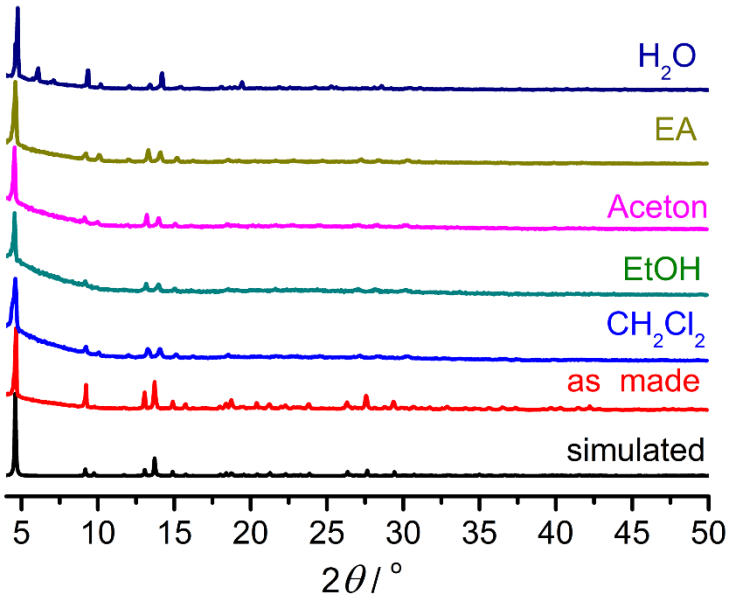

Fig. S8. (a) the TGA data of as-made **MAC-11** and **MAC-13** (the first step weigh loss of **MAC-11** agrees well with the weight loss of lattice water theoretically calculated from molecular weight, while **MAC-13** is not. It could be ascribed to the severe disorder of the lattice water in **MAC-13** that causes the difference between the TGA data and the molecular weight); (b) the TGA data of activated **MAC-11** and **MAC-13**.

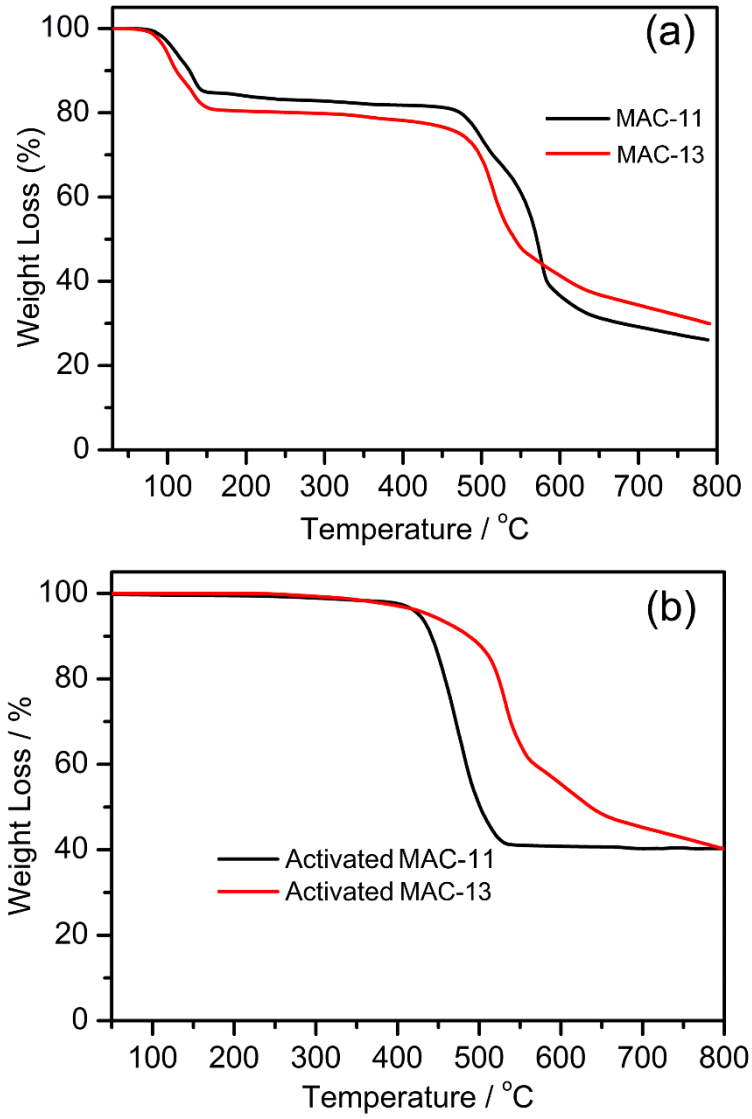

Fig. S9 the temperature-dependent PXRD patterns of **MAC-13** (phase transformation: 2θ = ~4.6 ° shifts to ~5.9° and then shifts back to 5.3° in water solution after **1** h)

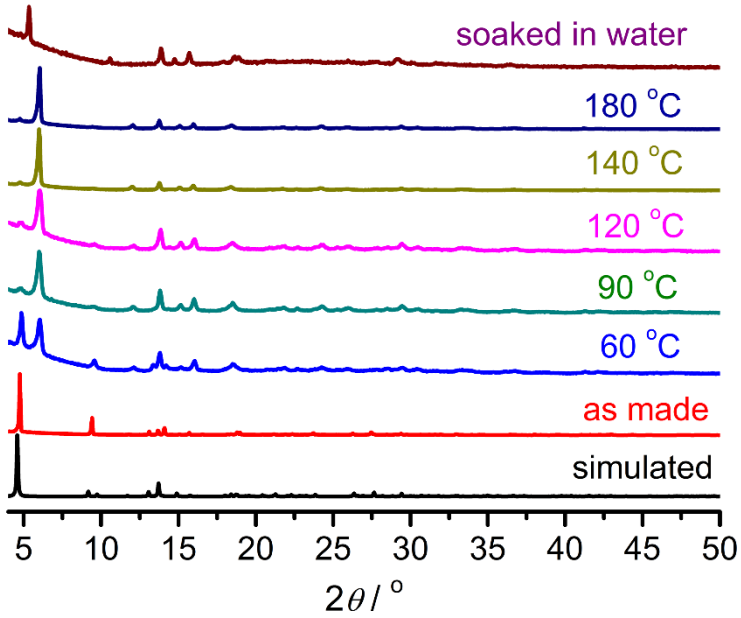

Fig. S10. the temperature-dependent PXRD patterns of **MAC-14** (the diffraction peak at 2θ = ~4.6 ° slightly shifts to 2θ = ~4.9°. The shift is much smaller than that of **MAC-11**)

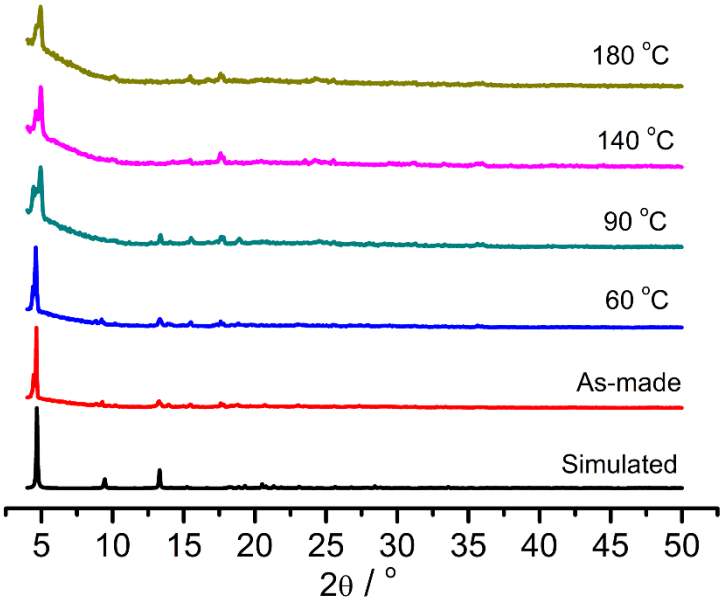

Fig. S11. The excitation and emission spectra of **MAC-11**

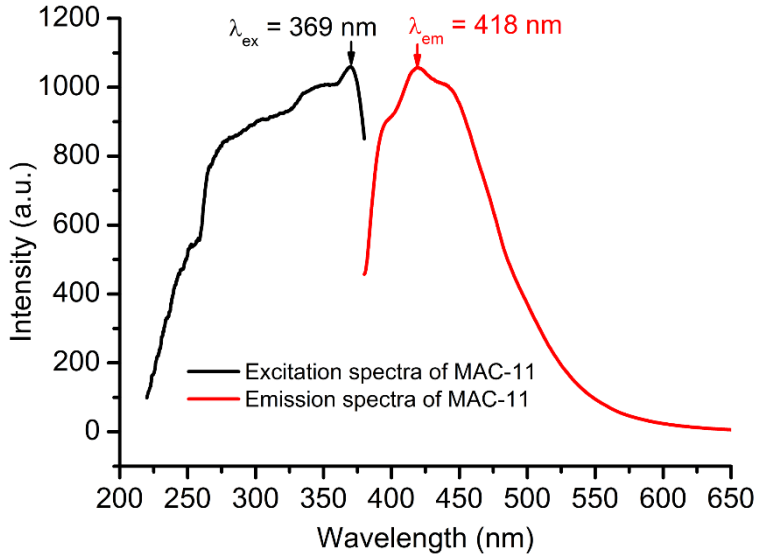

Fig. S12. The emission spectra of 2D layer [Zn(dmtrz)(HCOO)] (a), H_2L1 (b), their mixture (c) and MAC-14 before and after heated at 90 °C (λ_{ex} = 369 nm)

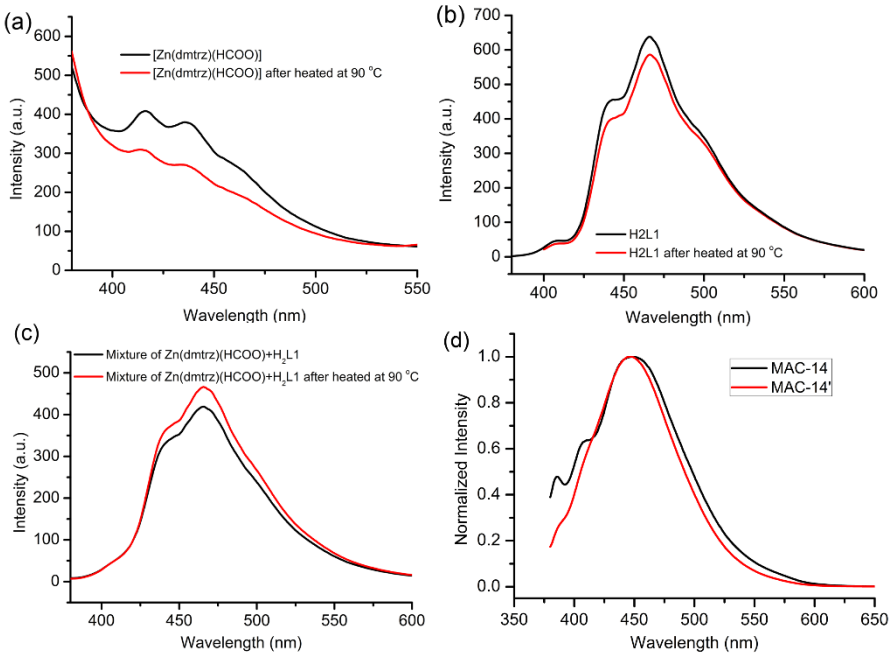

Fig. S13. (a) The FT-IR spectra of MAC-11 and MAC-11' showing the disappearance of the vibration band at 1675 cm^{-1}; (b) the FT-IR spectra of MAC-13 and MAC-13' showing the similar change of the carboxylate groups as that of MAC-11 on the vibration band; (c) the FT-IR spectra of MAC-14 and MAC-14', indicating that there is no obvious change on the vibration band of carboxylate group.